IEEE Photonics Journal
An IEEE Photonics Society Publication

Open Access

Photodetection of Infrared Photodetector Based on Surrounding Barriers Formed by Charged Quantum Dots

Volume 7, Number 3, June 2015

Hongmei Liu
Jianqi Zhang
Zhixiang Gao
Yunlong Shi

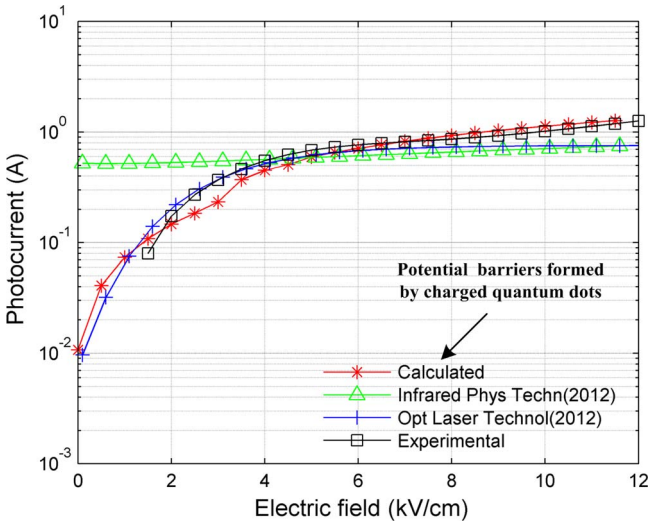

DOI: 10.1109/JPHOT.2015.2432076
1943-0655 © 2015 IEEE

IEEE photonics SOCIETY

IEEE

Photodetection of Infrared Photodetector Based on Surrounding Barriers Formed by Charged Quantum Dots

Hongmei Liu,[1,2] Jianqi Zhang,[3] Zhixiang Gao,[1,2] and Yunlong Shi[1,2]

[1]Institute of Solid State Physics, Shanxi Datong University, Datong 037009, China
[2]Higher Education Key Laboratory of New Microstructure Function Materials, Shanxi Datong University, Datong 037009, China
[3]School of Physics and Optoelectronics Engineering, Xidian University, Xi'an 710071, China

DOI: 10.1109/JPHOT.2015.2432076

Manuscript received April 21, 2015; revised May 7, 2015; accepted May 7, 2015. Date of publication May 12, 2015; date of current version May 28, 2015. This work was supported in part by the National Natural Science Foundation of China (NSFC) under Grant 61307121, by the Shanxi Provincial Foundation for Returned Scholars under Grant 2012-Key2, and by the Launching Scientific Research Funds for Doctors under Grant 2012-B-04. Corresponding author: H. Liu (e-mail: lhm9898@163.com).

Abstract: The photodetection performance of the quantum dot infrared photodetector (QDIP) is always a hot topic. In this paper, a model is proposed for the photocurrent of the QDIP, which not only considers the influence of the potential barrier around quantum dot on the photoconductive gain but includes the contribution of the quantum efficiency as well, based on the current balance relationship under dark conditions. The corresponding calculated results show a good agreement with the measured data, and they are furthermore used to calculate the responsivity, which can provide the device designers with the theoretical guidance for the optimization of the detector and the improvement of the device performance.

Index Terms: Quantum dot infrared photodetector (QDIP), electron transport, photocurrent, potential barrier.

1. Introduction

The quantum dot infrared photodetector (QDIP) is a novel quantum dot nanostructure infrared photodetector, which attracts a wide attention due to its superior properties [1]–[3]. In 2001, Ryzhii and his co-workers proposed a device model of the QDIP by thinking about the continuous potential distribution and the thermal emission of the electrons [4], [5], which was used to estimate the photocurrent and the responsivity. In 2009, the device model was improved with the consideration of the contribution of the field-assisted tunneling emission of the electrons [6], and the corresponding results showed a good agreement with the measured data [7]. In 2010, Lin pointed out that the microscale transport and the nanoscale transport of the electrons coexist in the QDIP devices [8]. Based on this theory, Liu rebuilt the device models of the QDIP used to estimate the photocurrent, the responsivity and so on in 2012 [9], [10], and these models not only consider of the microscale electron transport and the nanoscale electron transport, but also include the influence of the thermal emission of the electrons, the field-assisted tunnelling emission and the continuous potential distribution. Through carefully observing these models above used to calculate the photodetection performance of the QDIP, we find that

these models only consider the contribution of the capture of the electrons from the potential well of the quantum dot. In fact, back in 2008, Chien and Mitin *et al.* pointed out that the capture process of the electrons was very complex, and further, its strong dependence on the potential barriers built by the charged quantum dot should be included in the performance analysis of the QDIP [11], [12]. Hence, in our paper, a physical model is developed by accounting for the influence of the potential barriers built by the charged quantum dot on the photoconductive gain and the contribution of the quantum efficiency based on the dark current balance relationship. This model not only can theoretically predict and estimate the photodetection performances of the QDIP such as the photocurrent and the responsivity, but can also provide device designers with the theoretical guidance and the experimental verification in optimizing the device and improving the device performance, which lays the foundation of the wide application of the QDIP in the future.

2. Theory

In this section, the photocurrent model of the QDIP is built by considering the contribution of the quantum efficiency and the photoconductive gain, and then based on which, we further derive the responsivity expression of the QDIP.

2.1. Photocurrent

As we all know, the QDIP is mainly composed of the excited region including the barrier layers and the repetitive quantum dot composite layers, the top contact layer, and the bottom contact layer [2], [10]. When the infrared light irradiates the excited region of the photodetector, the electron transition will take place between the ground state and the excited state, which will change the conductivity of the QDIP, and the photocurrent will be formed in the circuit if a biased voltage is applied to the both ends of the photodetector, which can be written as

$$I_{\text{photo}} = e\Phi_s \eta g_p A \tag{1}$$

where e is the electron charge, Φ_s is the incident photo flux density on a detector, η is the quantum efficiency, and g_p is the photoconductivity gain, A is the area of the photodetector.

In the QDIP, the photoconductive gain g_p can be obtained as the ratio of the capture time of the electrons (lifetime of the electrons) to the transition time of the electrons across the whole detector, and in the other hand, under the condition that the capture probability is small and the transit time across one period of the quantum dot composite layer is considerably smaller than the recombination time from an extended state back into a quantum dot, the photoconductive gain is also determined by the capture probability and the number of quantum dots layers [2], [9], which can be written as

$$g = \frac{\tau_{\text{cap}}}{\tau_{\text{trans}}} = \frac{1}{Kp_k} \tag{2}$$

where τ_{cap} is the lifetime of the electrons, τ_{trans} is the transition time across the quantum dot infrared photodetector, K is the total number of the quantum dot composites layers, and p_k is the neutral capture probability and can be written as [6]

$$P_k = P_{0k} \frac{N_{QD} - \langle N \rangle}{N_{QD}} \exp\left(- \frac{e^2 \langle N \rangle \pi \sqrt{\pi}}{2\varepsilon_0 \varepsilon_r a_{QD} kT} \right) \tag{3}$$

where P_{0k} is the capture probability for the uncharged quantum dots, and a_{QD} is the lateral dimension of the quantum dot, e is the electron charge, k is the Boltzmann constant, T is the temperature, $\langle N \rangle$ is the average number of electrons in a quantum dot, and N_{QD} is the maximum of the number of electrons that can occupy a quantum dot.

Substituting (3) into (2), we get [9]

$$g_p = \frac{N_{QD}}{KP_{0k}(N_{QD} - \langle N \rangle)\exp\left(-\frac{\pi\sqrt{\pi}e^2\langle N \rangle}{2\varepsilon_r\varepsilon_0 a_{QD}kT}\right)}. \tag{4}$$

In the photoconductive gain above [see (4)], the photoconductive gain strongly depends on the capture probability of electrons, namely, it is determined by the capture of the electrons from the potential well of the quantum dot. In fact, in 2008, it was pointed out that the capture of the electrons has a heavy dependence on the potential barriers built by the charged quantum dot. Hence, in our model, the influence of the potential barriers built by the charged quantum dots is considered. To be specific, in the calculation of the photoconductive gain as (2) shown, the transition time across the quantum dot infrared photodetector can be obtained by $(K+1)L/v_d$. Here, $(K+1)L$ is the length of the quantum dot infrared photodetector, v_d is the drift velocity of the electrons. According to the characteristics of the electron motion under the different electric field, the drift velocity can be calculated by Monte Carlo method at the low electric field, and at the high electric field, it can be calculated as [13], [14]

$$v = \mu E\left(1 + \left(\frac{\mu E}{v_s}\right)^2\right)^{-\frac{1}{2}} \tag{5}$$

where v_s is the saturation velocity of electrons, E is the electrical field intensity, and μ is the mobility of electrons.

In the QDIP, the capture of electrons will be repulsed by charged quantum dot, and it can be realized via the tunneling through the surrounding barrier or the thermal excitation above the barrier [11], [12]. Thus, it is this capture process of electrons that leads to the longer lifetime of the electrons, and furthermore, this lifetime depends on the height of the potential barriers built by the in-dot charge, which can be written as [11], [12], [15]

$$1/\tau_{\text{cap}} = \pi N_{\text{dot}} a^3 \tau_\varepsilon^{-1} \exp\left(-\frac{eV_m}{kT}\right) \tag{6}$$

where N_{dot} is the dot concentration, a is the quantum radius, V_h is the height of the potential barrier around the dot, and τ_ε is the electron-phonon relaxation time which corresponds to the transitions from conducting states to the localized QD states [16], and it can be written as

$$\tau_\varepsilon = \frac{1}{W} = \frac{\pi^2 h^4 c_1}{(m^*)^{\frac{3}{2}}\Xi^2 kT(2E_e)^{\frac{1}{2}}} \tag{7}$$

where m^* is the effective mass of the electrons, E_e is the energy of the electron, Ξ is the deformation potential constant, and c_1 is the longitudinal elastic constants which can be obtained by the multiplying the density ρ by the velocity of the photon v_s^*.

Substituting (6), (7) into (2), we can get the gain, which can be shown as

$$g_p = \frac{(m^*)^{\frac{3}{2}}\Xi^2 kT(2E_e)^{\frac{1}{2}} v_d}{\pi^3 h^4 c_1 N_{\text{dot}} a^3 \exp\left(-\frac{V_h}{kT}\right)(K+1)L}. \tag{8}$$

In the QDIP, the quantum efficiency η is related to the absorption coefficient, which can be approximated by $\eta \approx \alpha KL$, where α is the absorption coefficient, which can be estimated using the following equation [2], [17]:

$$\alpha = \frac{\delta\langle N \rangle \sum_{QD}}{L} \tag{9}$$

where δ is the electron capture cross section coefficient and is adjusted to meet experimental comparison, $\sum_{QD}$ is the quantum dot density in a layer, and L is the thickness of the quantum

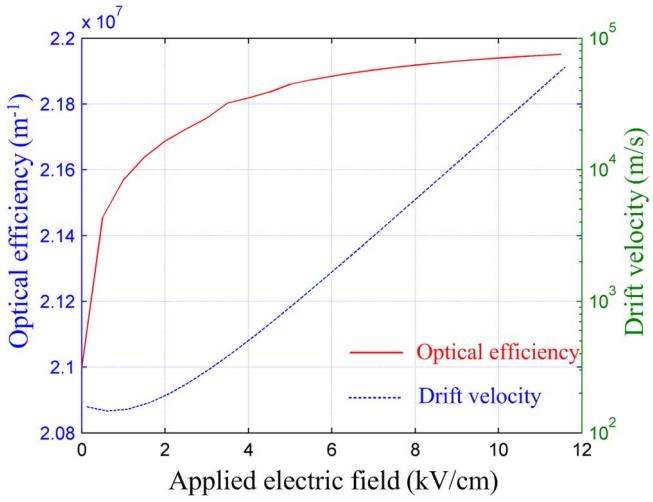

Fig. 1. Optical efficiency and drift velocity.

dot layer. Based on the expression of the absorption coefficient [see (9)], the quantum efficiency can be written as

$$\eta = \delta \langle N \rangle K \sum_{QD} \tag{10}$$

where $\langle N \rangle$ is the average electron number in a quantum dot which can be calculated by solving the dark current balance relationship [9], [10], [18]; furthermore, it can be written as

$$2ev_d \left(\frac{m^* k_B T}{2\pi\hbar^2}\right)^{3/2} \exp\left(-\frac{E_{a,\text{micro}} + E_{a,\text{nano}}}{kT}\right) = A^* T^2 \frac{\Theta}{\langle N \rangle} \exp\left[e\frac{V + V_d - (\langle N \rangle / N_{QD}) V_{QD}}{(K+1)kT}\right] \tag{11}$$

where v_d is the drift velocity of electrons, m^* is the effective mass of the electron, $\hbar$ is the reduced Planck constant, $E_{a,\text{micro}}$ and $E_{a,\text{nano}}$, respectively, represent the activation energies under the microscale and the nanoscale transport, V is the applied voltage, A^* is the Richardson constant, and the other parameters Θ V_{QD} and V_d are related to the structure parameters and the materials parameters.

Substituting (10), (8) into (1), then we can get the expression of the photocurrent which can be shown as

$$I_{\text{photo}} = \frac{e\Phi_s A \delta \langle N \rangle K \sum_{QD} (m^*)^{\frac{3}{2}} \Xi^2 kT (2E_e)^{\frac{1}{2}} v_d}{\pi^3 h^4 c_1 N_{\text{dot}} a^3 \exp\left(-\frac{V_b}{kT}\right)(K+1)L}. \tag{12}$$

Based on the photocurrent above, the current responsivity of the QDIP can be written as

$$R_i = \frac{I_{\text{photo}}}{\Phi_s h v_0} = \frac{\delta e g_p \langle N \rangle \sum_{\text{QD}} K}{h v_0} \tag{13}$$

where v_0 is the frequency of the incident infrared light.

3. Results

In this section, the photodetection performances of the QDIP as function of the electric field are simulated and calculated, the corresponding results are shown in Figs. 1–4. Here, it is worth mentioning that the comparison between our current works and the previous work [9], [10] is given in Fig. 3, because the advantages of the photoconductive gain in our paper can directly reflect in the photocurrent of the QDIP. Table 1 shows the values of the parameters used to calculate and simulate the photocurrent, the responsivity of the QDIP [1]–[21].

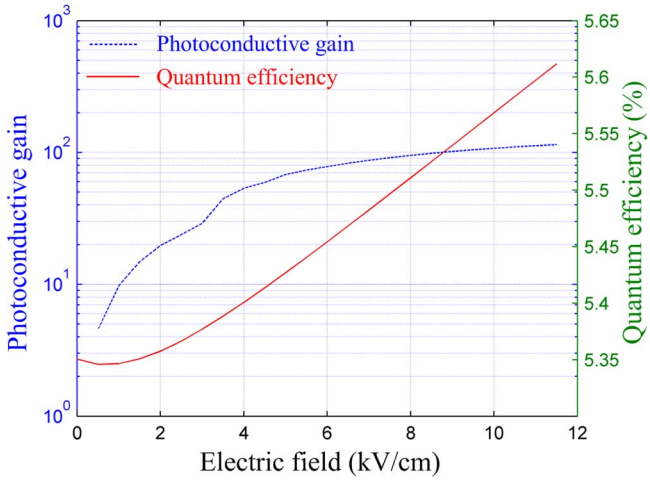

Fig. 2. Photoconductive gain and quantum efficiency.

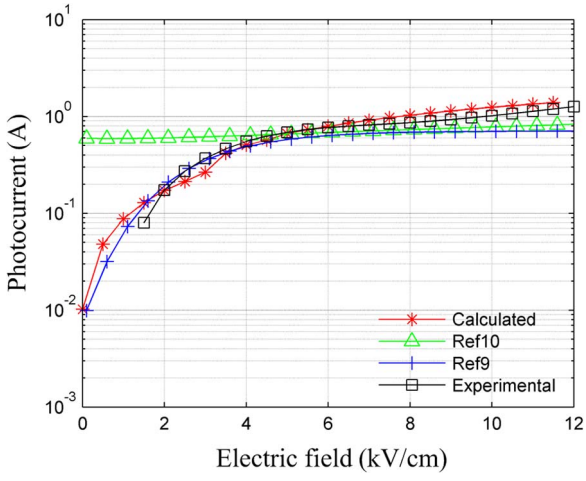

Fig. 3. Photocurrent as a function of electric field.

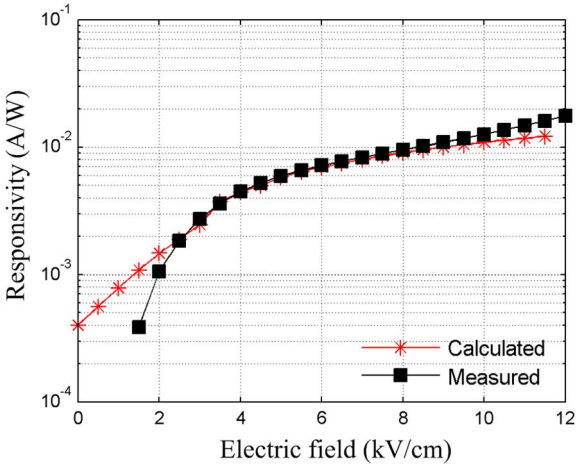

Fig. 4. Responsivity of the QDIP at 80 K.

TABLE 1

Parameters of QDIP

E_0=1.62kV/cm	m^*=0.5m_e	$E_{0,nano}$=224.7meV	a_{QD} = 22nm,30nm
β =2.79meVcm/kV	Ξ = 6.5eV	$E_{0,micro}$=34.6meV	T = 80K,100K
v_s^* = 3240m/s	ρ = 5.667kg/m^3	ε_r = 12.8	E_e = 0.027eV
$\Sigma_{QD} = 5\times10^{10} cm^{-2}$	N_{QD} = 8	L = 31.5nm,59nm	$\Sigma_D = 0.3\Sigma_{QD}$
$G_{t0} = 5\times10^{13} S^{-1}$	$G_0 = 10^{11} S^{-1}$	K=10	$\Phi_s = 8\times10^{17} cm^{-2}$
μ =1000$cm^2V^{-1}s^{-1}$	$v_s = 1\times10^7$cm/s	A=100×100μm^2	P_{ok} = 1

Fig. 1 shows the dependences of the optical absorption and the drift velocity on the electric field density. In this figure, the red curve describes the optical absorption efficiency of the QDIP, which corresponds to the y-axis on the left, the other blue curve is on half of the drift velocity of the electrons, and its corresponding y-axis is on the right of Fig. 1. The two curves have the increase trends with the increase of the applied electric field. Taking the curve marked as "optical efficiency" for example, the optical absorption efficiency is 2.09×10^7 m^{-1} at the electric field 1 kV/cm, and it increases to 2.17×10^7 m^{-1} when the electric field is increased to 10 kV/cm, which is higher than that at 1 kV/cm. This increase of the optical absorption efficiency shows the dependence of the optical absorption efficiency on the electric field. Similarly, the electric field also has a big effect on the drift velocity of the electrons. When the electric field changes from 1 kV/cm to 10 kV/cm, the drift velocity also has a corresponding increase from 8.04×10^3 m/s to 7.07×10^4 m/s, which directly displays the increase trend of the drift velocity with the increase of the electric field. In addition, it can be noted that this drift velocity change trend also shows a floating up and down at about 4 kV/cm, which is ascribed to the change of the drift velocity calculation method (Monte Carlo method below 4 kV/cm). Of course, based on the calculation of the drift velocity, the following calculations of the gain, the photocurrent, and the responsivity also show similar floating.

Fig. 2 not only shows the calculated results of the quantum efficiency of the QDIP, but also describes the change of the photocurrent gain of the QDIP within the electric field of 0–12 kV/cm. In this figure, the photoconductive gain corresponds to the left y-axis, and the y-scale of the quantum efficiency is in the right. Look at the curve of the photoconductive gain, the photoconductive gain is 18.76 when the electric field density is 2 kV/cm, and it sharply increases to 107.58 at the 10 kV/cm, which is about 4 times higher than that at 2 kV/cm. The similar increase of the gain can also be seen in literature [2], [14]. Looking at the curve of the quantum efficiency based on the y-axis in the right, we find that the quantum efficiency clearly increases from 5.37% to 5.57% when the electric field changes from the 2 kV/cm to 10 kV/cm. This increased trend of the quantum efficiency depends on the influence of the electric field density on the tunneling emission.

Fig. 3 represents the photocurrent of the QDIP within 0–12 kV/cm. In this figure, the curve with "$*$" describes the photocurrent data of the QDIP at the temperature 100 K from our model, the curve with "△" depicts the photocurrent values based on the constant photoconductive gain from Ref[10], the curve with "+" represents the photocurrent data from [9], where it is assumed that the photoconductive gain strongly depends on the capture probability of the electrons [see (4)]. The final one with "□" represents the measured photocurrent values [20]. Let's make a comparison between these photocurrent curves, it can be found that these curves are very close each other at high electric field, but have the big differences at low electric field. Specially, the photocurrent curve from [10] is bigger than that from the other curves at the low electric field, which is ascribed to the operation that the dependence of the photoconductive gain on the electric field is ignored in the calculation of the photocurrent. Compared with the experimental data,

it shows the lowest computational accuracy in the estimation of the photocurrent within the three methods in Fig. 3 (respectively corresponding to the method from [9], [10], and our manuscript). Let us make a comparison between the red curve with "$*$" from our model and the blue curve with "$+$" from [9]. Under the low electric field (0–2 kV/cm), the two curves only have a light difference, but when the electric field increases, the photocurrent values from our model become increasingly higher than that from [9] with the electric field 6 kV/cm as the starting point. If compared with the experimental data, those values from our model show a better agreement with the experimental data due to this difference, which not only show the calculation from our model is more previous than that from [9], but also directly verify the correctness and the validity of our model. In addition, it can be seen from Fig. 3 that the four curves have the same characteristics, that is, the photocurrent increases with the increase of the electric field. Let us take the curve marked as "Calculated" for example, the photocurrent changes from 0.14 A to 1.13 A when the electric field density changes from 2 kV/cm to 10 kV/cm, namely, the photocurrent at 10 kV/cm is about six times higher than that at 2 kV/cm. Of course, the similar increase trend can also be seen in the other curves. The nature of the increase can be explained as follows: when the electric field density is increased, the motion of the electrons speeds up, thus more and more electrons can be used to form the photocurrent of the QDIP as a result of the decrease in the capture probability. In the end, the large photocurrent is obtained.

Based on the calculated photocurrent values above, the corresponding results of the responsivity of the QDIP are shown in Fig. 4. The curve with "$*$" describes the calculated responsivity results of the QDIP according to our model at the 80 K, and the other curve with "■" stands for the experimental measured data of the responsivity at the same temperature [21]. Obviously, our calculated responsivity values show a good agreement with the measured data, which proves the rightness of our models again. In addition, the two curves have the same changing trends, that is the increase of the responsivity with the increase of the electric field. Taking our calculated responsivity values (corresponding to the curve "calculated") for example, when the electric field density is at 2 kV/cm, the responsivity is 1.61×10^{-3} A/W and it reaches 1.08×10^{-2} A/W when the electric field density is at 10 kV/cm, which is about an order of magnitude bigger than that at 2 kV/cm. The similar increased trend can also be seen on the other curve marked as "measured." This increase trend of the responsivity with the increase of the electric field density can be essentially ascribed to the increase of photocurrent with the increase of the electric field density.

4. Conclusion

In this paper, the photocurrent of quantum dot infrared photodetector is simulated and calculated by considering the influence of the potential barrier around quantum dots on the photoconductive gain and the contributions of the quantum efficiency. The corresponding results are compared with the measured data to show the validity and rightness of the calculated method in our paper. Based on these photocurrent results, the calculated results of the responsivity of the QDIP are also further given. These calculated results shows the strong dependence of the electric field, which can provide with the method to obtain the optimized performance of the QDIP, and make the contribution to the wide application of the QDIP in the commercial field, defense fields, and so on.

References

[1] G. Gu, J. Vaillancourt, and X. Lu, "Analysis of near-field components of a plasmonic optical antenna and their contribution to quantum dot infrared photodetector enhancement," *Opt. Exp.*, vol. 22, no. 21, pp. 24 970–24 976, Oct. 2014.
[2] P. Martyniuk and A. Rogalski, "Quantum-dot infrared photodetectors: Status and outlook," *Progr. Quantum Electron.*, vol. 32, no. 3/4, pp. 89–120, 2008.
[3] V. Ryzhii, "The theory of quantum-dot infrared phototransistors," *Semicond. Sci. Technol.*, vol. 11, no. 5, pp. 759–761, May 1996.
[4] V. Ryzhii, "Physical model and analysis of quantum dot infrared photodetectors with blocking layer," *J. Appl. Phys.*, vol. 89, no. 9, pp. 5117–5224, May 2001.

[5] V. Ryzhii, I. Khmyrova, V. Pipa, V. Mitin, and M. Willander, "Device model for quantum dot infrared photodetectors and their dark-current characteristic," *Semicond. Sci. Technol.*, vol. 16, no. 5, pp. 331–338, May 2001.
[6] A. D. Stiff-Robert, "Contribution of field-assisted tunneling emission to dark current in InAs–GaAs quantum dot infrared photodetectors. *IEEE Photon. Technol. Lett.*, vol. 16, no. 3, pp. 867–869, Mar. 2004.
[7] P. Martyniuk and A. Rogalski, "Insight into performance of quantum dot infrared photodetectors," *Bull. Pol. Acad. Sci. Tech. Sci.*, vol. 57, no. 1, pp. 103–116, Mar. 2009.
[8] L. Lin *et al.*, "Sequential coupling transport for the dark current of quantum dots-in-well infrared photodetectors," *Appl. Phys. Lett.*, vol. 97, no. 19, Nov. 2010, Art. ID. 193511.
[9] H. Liu and J. Zhang, "Physical model for the dark current of quantum dot infrared photodetectors," *Opt. Laser Technol.*, vol. 44, no. 5, pp. 1536–1542, Jul. 2012.
[10] H. Liu, H. Liu, and J. Zhang, "Performance investigations of quantum dots infrared photodetector," *Infrared Phys. Technol.*, vol. 55, no. 4, pp. 320–325, Jul. 2012.
[11] V. Mitin, A. Sergeev, N. Vagidov, and S. B. Irner, "Improvement of QDIP performance due to quantum dots with built-in charge," *Infrared Phys. Technol.*, vol. 50, pp. 84–88, Jul. 2013.
[12] A. Sergeev, V. Mitin, and M. Stroscio, "Quantum-dot photodetector operating at room temperature: Diffusion-limited capture," *Phys. B, Condens. Matter*, vol. 316/317, pp. 369–372, May 2002.
[13] A. Carbone, R. Introzi, and H. Liu, "Photo and dark current noise in self-assembled quantum dot infrared photodetectors," *Infrared Phys. Technol.*, vol. 52, no. 6, pp. 260–263, Nov. 2009.
[14] H. Lim *et al.*, "Gain and recombination dynamics of quantum-dot infrared photodetectors," *Phys. Rev. B, Condens. Matter*, vol. 74, no. 20, Nov. 2006, Art. ID. 205321.
[15] V. Mitin, A. Sergeev, L.-H. Chien, and N. Vagidov, "Monte-Carlo modeling of photoelectron kinetics in quantum-dot photodetectors," in *Proc. IEEE Int. Workshop Comput. Electron.*, 2009, pp. 1–4.
[16] C. Jacoboni and L. Reggiani, "The Monte Carlo method for the solution of charge transport in semiconductors with applications to covalent materials," *Rev. Mod. Phys.*, vol. 55, no. 3, pp. 645–647, Jul. 1983.
[17] I. Mahmoud Imbaby, A. Konber Hussien, and S. El Tokhy Mohamed, "Performance improvement of quantum dot infrared photodetectors through modeling," *Opt. Laser Technol.*, vol. 42, no. 8, pp. 1240–1249, Nov. 2010.
[18] H. Liu, Q. Tong, G. Liu, C. Yang, and Y. Shi, "Performance characteristics of quantum dot infrared photodetectors under illumination condition," *Opt. Quantum Electron.*, vol. 47, no. 3, pp. 721–733, Mar. 2015.
[19] G. Satyanadh, R. P. Joshi, N. Abedin, and U. Singh, "Monte Carlo calculation of electron drift characteristics and avalanche noise in bulk InAs," *J. Appl. Phys.*, vol. 91, no. 3, pp. 1331–1338, Feb. 2002.
[20] S. Lin, Y. Tsai, and S. Lee, "Comparison of InAs/GaAs quantum dot infrared photodetector and GaAs/(AlGa)As superlattice infrared photodetector," *Jpn. J. Appl. Phys.*, vol. 40, no. 12A, pp. L1290–L1292, Dec. 2001.
[21] G. Ariyawansa, S. G. Matsik, A. G. U. Perera, X. H. Su, and P. Bhattacharya, "Tunneling quantum dot sensors for multi-band infrared and terahertz radiation detection," in *Proc. IEEE Sensors Conf.*, 2007, pp. 503–506.